



## Electrochemical micromachining of Hastelloy B-2 with ultrashort voltage pulses

Joseph J. Maurer<sup>a</sup>, Jonathan J. Mallett<sup>a</sup>, John L. Hudson<sup>a</sup>, Steven E. Fick<sup>b</sup>,  
Thomas P. Moffat<sup>b</sup>, Gordon A. Shaw<sup>b,\*</sup>

<sup>a</sup> University of Virginia, Department of Chemical Engineering, 102 Engineers' Way, Charlottesville, VA 22904, United States

<sup>b</sup> National Institute of Standards and Technology, 100 Bureau Dr, Gaithersburg, MD 20878, United States

### ARTICLE INFO

#### Article history:

Received 17 July 2009

Received in revised form 1 September 2009

Accepted 3 September 2009

Available online 8 September 2009

#### Keywords:

Micromachining

Nickel-based superalloy

Etching

Microstructures

Ultrashort voltage pulses

### ABSTRACT

Electrochemical micromachining (ECMM) with ultrashort voltage pulses, a maskless all-electrochemical micro and nanofabrication technique, was used to fabricate microstructures on a corrosion resistant nickel-based superalloy, Hastelloy B-2,<sup>1</sup> whose work hardening behavior makes it difficult to machine on the macroscale. This work presents a viable, strain-free micromachining strategy for this technologically important material. ECMM was used to machine microstructures to depths of 3  $\mu\text{m}$  and 10  $\mu\text{m}$ , and the resolution of the machining was found to be dependent on the duration of the nanoscale pulses. Microstructures were also machined to 100  $\mu\text{m}$  depths, demonstrating the potential for the fabrication of high aspect ratio features using this technique. The ECMM was performed utilizing an apparatus consisting of standard electrochemical equipment combined with a custom electrical circuit that was constructed easily and at low cost.

Published by Elsevier Ltd.

### 1. Introduction

Electrochemical micromachining (ECMM) with ultrashort voltage pulses is a maskless, all-electrochemical method used for the creation of microstructures and nanostructures on conductors and semiconductors. This technique was first developed by Schuster et al. [1,2] and has been used to machine microscale and submicroscale structures into a variety of workpiece materials including Cu [2,3], Au [4], stainless steel [5], Ni [3,6], polypyrrole [7], and p-Si [2,8,9]. The ECMM of p-Si substrates was also used as method for selective Cu metallization of p-Si surfaces [9].

In ECMM with ultrashort voltage pulses, a microscale tool electrode is used to machine its imprint into a workpiece electrode. When the transient, ultrashort voltage pulses are combined with microscale tools, the localized negative pattern of the tool is transferred onto the workpiece. To illustrate the effect of the transient voltage pulses on the machining, consider the schematic of the ECMM process shown in Fig. 1. When a potential is applied between

the tool and the workpiece, the charging of the double-layer (DL) capacitance  $C_{DL}$  occurs at both electrodes. For each region  $R$ , the localized time constant for the charging of the DL capacitance,  $\tau_{DL}$ , can be approximated as the product of  $C_{DL}$  and the solution resistance  $R$ . ECMM with ultrashort pulses works by taking advantage of the fact that  $R$  is proportional to the distance through the solution, thus making  $\tau_{DL}$  distance dependent. This means longer current paths, such as illustrated by  $R_{Long}$  in Fig. 1, have a larger time constant associated with the charging of their DL capacitance, than shorter current paths, such as illustrated by  $R_{Short}$  in Fig. 1. Thus, the time constant for a long path is greater than that of a short path, or  $\tau_{Long} > \tau_{Short}$ . If ultrashort voltage pulses with a pulse duration  $\tau_{Pulse}$  that is less than  $\tau_{Long}$  are then applied to the tool, the DL of the region associated with the long current path will not have time to charge, allowing only those paths whose  $\tau_{DL} < \tau_{Pulse}$  to polarize enough to initiate dissolution. This means the lateral extension of the anodic dissolution reaction on the workpiece's surface can be controlled by both the size of the tool and the duration of the voltage pulses used. In this fashion, ECMM with ultrashort voltage pulses can be used to control the size of micromachined features simply by using voltage pulses of different duration.

Hastelloy is a trade name for a group of nickel-based superalloys manufactured by Haynes International, Inc. Hastelloy substrates are corrosion resistant [10–12], industrially relevant as a material for reactors, pipes, and pumps [10,12], and could potentially be used as a microreactor material [13]. Hastelloy B-2 is a Ni (68% atomic fraction)–Mo (28% atomic fraction) alloy that also contains

\* Corresponding author. Tel.: +1 301 975 6614; fax: +1 301 417 0514.

E-mail address: [Gordon.Shaw@nist.gov](mailto:Gordon.Shaw@nist.gov) (G.A. Shaw).

<sup>1</sup> This article is authored by employees of the U.S. federal government, and is not subject to copyright. Commercial equipment and materials are identified in order to adequately specify certain procedures. In no case does such identification imply recommendation or endorsement by the National Institute of Standards and Technology, nor does it imply that the materials or equipment identified are necessarily the best available for the purpose.

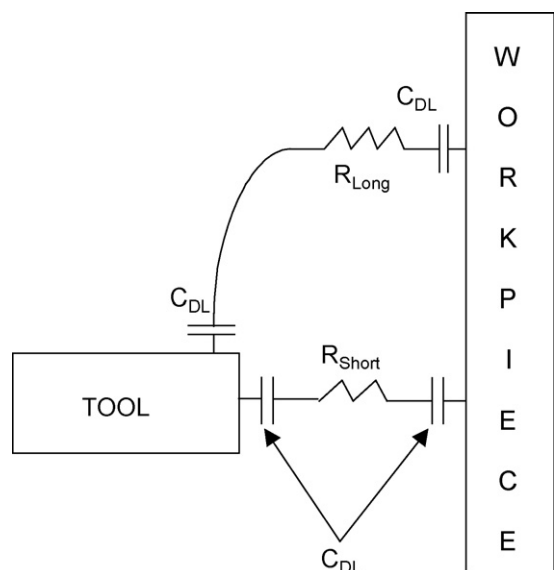


**Fig. 1.** A schematic of the ECMM with ultrashort voltage pulses process illustrating the DL capacitances of both electrodes and two paths of current from the tool to the workpiece. In this schematic, the dependence of effective solution resistance  $R$  on distance is shown as  $R_{\text{Long}} > R_{\text{Short}}$ . The time constant associated with the DL capacitance is  $\tau_{\text{DL}} = R \times C_{\text{DL}}$ . This means  $\tau_{\text{Long}} > \tau_{\text{Short}}$  and that the charging of the DL capacitance associated with long paths can be eliminated by choosing a pulse duration for the machining such that  $\tau_{\text{pulse}} < \tau_{\text{Long}}$ . This is the principle of ECMM with ultrashort pulses. This figure and argument follow that of Trimmer et al. [3] and Allongue et al. [8].

smaller amounts of Fe, Cr, Si, Co, Mn, P, S, and V and is known for its strong corrosion resistance in reducing acids [10,12]. The high concentration of Mo also makes Hastelloy B-2 stronger than pure Ni [10] and more susceptible to work hardening during traditional machining and welding processes.

The effect of Mo addition to nickel-based superalloys on electrochemical reactivity has been extensively studied. Uhlig et al. [14] showed the corrosion rate of Ni–Mo alloys in deaerated HCl was dependent on the fraction of Mo with alloys higher in Mo (up to 20%) demonstrating the lowest corrosion rates. Horvath and Uhlig [15] demonstrated the addition of Mo to Ni was also found to reduce pitting corrosion in 0.1 mol/L NaCl solutions with no pitting occurring after the addition of 6.8% Mo. Luo and Ives [16] showed that Ni–Mo alloys with 5% Mo had fewer and shallower pits than Ni alone at the same applied potential in 0.5 mol/L  $\text{Na}_2\text{SO}_4 + 0.1$  mol/L NaCl and indicated that adding Mo to Ni has the same effect as decreasing the potential. At high Mo concentrations such as found in Hastelloy B-2, Ni–Mo alloys exhibit dissolution behavior analogous to pure Mo [10]. Surface analytical studies conducted by Lu and Clayton on Mo [17] reveal the important role of the Mo in controlling the passivation of Ni in high Cl. As anodic potential is increased Mo undergoes an abrupt transition from passive to transpassive dissolution. The transpassive dissolution regime of Mo is evident at easily accessible potentials, thus Ni–Mo alloys are ideal for ECMM as negligible etching occurs when near open circuit, while rapid dissolution can be activated by stepping the potential into the transpassive regime.

In this work, the ECMM of Hastelloy B-2 is performed by pulsing the tool to potentials that will initiate localized transpassive dissolution of this Ni–Mo alloy. For the ECMM, an experimental setup with a custom electrical circuit was used with otherwise standard electronic and electrochemical equipment. This setup was different than in previous ultrashort pulse ECMM work [3,9]. The ECMM of Hastelloy B-2 using this experimental setup demonstrated a low cost method for the strain-free fabrication of microstructures into this industrially relevant material.

## 2. Experimental

The Hastelloy B-2 workpiece electrodes were cut from ingots (Haynes International, Inc.) and were polished on a single side with 4000 grit SiC paper. Tool electrodes were made from tungsten wires (99.99% Alfa Aesar) with a diameter of 100  $\mu\text{m}$ . The tools were fabricated by reducing one end of the wire to a smaller diameter via electrochemical etching in 1 mol/L NaOH (Fisher Scientific) using an AC power supply at 8 V. This tool was then insulated by covering its shaft with wax (Apiezon Type W) reducing the exposed tool area to approximately a few hundred microns.

The reference electrode was a quasi-reference Pd/H<sub>2</sub>, which is +50 mV vs. SHE, prepared by applying a potential of 2.5 V between a Pd and a Pt wire immersed in 1 mol/L H<sub>2</sub>SO<sub>4</sub> solution [18]. The counter electrode was a Pt wire (Alfa Aesar). The electrolytes used in the machining were aerated 1 mol/L and 2 mol/L HCl supplied as 37% HCl by mass (JT Baker) diluted to the appropriate concentration with deionized water.

Potentiodynamic scans were performed to determine the electrochemical behavior of Hastelloy B-2 electrodes. The scans were performed with a potentiostat (Gamry Instruments Ref 600) using a Hastelloy B-2 working electrode, a Pt counter electrode, and either an H<sub>2</sub>/Pd, or a saturated calomel reference electrode in 1 mol/L HCl. A nitrogen sparge was performed before acquiring the data shown. All potentials are reported vs. H<sub>2</sub>/Pd.

The apparatus was built at the National Institute of Standards and Technology in Gaithersburg, MD. A block diagram of the experimental apparatus is shown in Fig. 2. The setup was constructed on an Olympus 2000TE inverted optical microscope. A crossed roller bearing stage from Asylum Research was attached above the objective, and permitted coarse positioning of the tool electrode near the workpiece electrode. The tool was soldered to a circuit board and mounted to the coarse positioning stage magnetically, as was a glass microscope slide modified to provide a well approximately 1 mL in volume for containing the electrolyte. The workpiece was attached to a New Focus miniature precision stage to control its position in  $x$ ,  $y$ , and  $z$ . Fine motion control was achieved using Pico-motor actuators controlled using a New Focus Model 8572 Ethernet controller and custom written software in Igor Pro. This configuration permits the viewing and imaging of the machining process in situ as well as providing independent control of the relative motion of the tool, workpiece, and microscope objective.

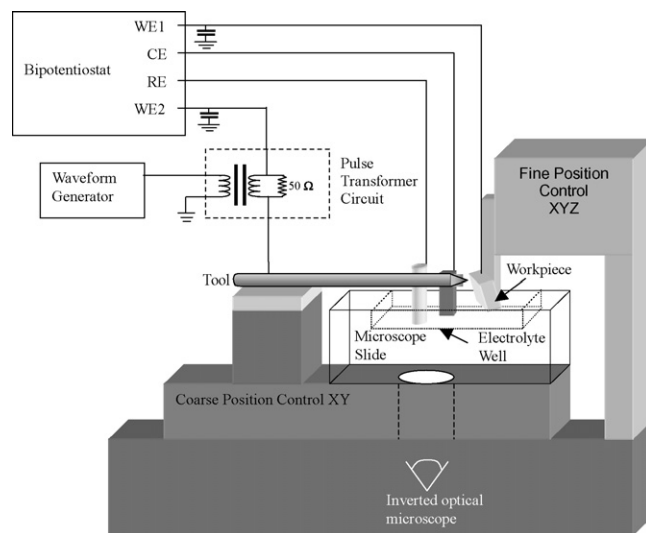


**Fig. 2.** A schematic of experimental apparatus used in the ECMM. The custom pulse transformer circuit was used with otherwise standard electronic and electrochemical equipment.

An electrical circuit was constructed that allowed the ECMM to be performed with standard electrochemical equipment. A Pine bipotentiostat (AFCBP1) was used to control DC potential at the tool, workpiece, reference, and counter electrodes. A wide band transformer (Coilcraft WB1-1) was used to superimpose ultrashort pulses generated by a LeCroy waveform generator (LW420) on the DC signals from the bipotentiostat as shown in Fig. 2. The 50  $\Omega$  resistor was used to match the output impedance of the waveform generator, thereby maximizing the amplitude of the pulse transmitted. The lowest frequency component of the pulses used was 1 MHz, which was well above the maximum bandwidth of the control system of the bipotentiostat. As a result, it behaved as a very high impedance device, and bypass capacitors were used to provide a low impedance path for the current necessary for the electrochemical reactions. This approach represents a simple, low cost method for creating an ECMM apparatus using equipment commonly available in an electrochemistry laboratory. We note, however, that care must be taken when the tool electrode is positioned near the workpiece. Since the position control in this prototype configuration is open loop, there is some danger of the tool and workpiece colliding, which can result in bending of the tip of the tool electrode.

Prior to the machining process, the tool was brought into close proximity with the workpiece, and then electrolyte was added to the well, immersing both the tip of the tool electrode and the workpiece electrode while maintaining control of the potential on each, preventing DC corrosion. Subsequently, the waveform generator was switched on to supply the requisite pulses to the tool in a duty cycle of 1:10. The workpiece was then moved toward the fixed tool electrode in discrete steps of 30 nm at 1-s intervals. The depth of the machined features is reported as the total distance advanced by the tool electrode during the stepping process. For the shallower features, this depth was checked using atomic force microscopy (AFM) on the features and the two values agreed to within approximately 25%. For the higher aspect ratio features, precision calipers were used to measure the thickness of the workpiece through which a hole was machined. As the material near the tool was dissolved from the workpiece, the progress of the machining reaction was observed through the inverted microscope. After the desired feature depth was reached, the tool electrode was withdrawn.

After machining, samples were removed from the electrolyte, rinsed thoroughly with deionized water, and air-dried. The machined features were then examined using a scanning electron microscope (SEM). Scanning electron micrographs of the machined features were taken using a Hitachi S-4700 Field Emission SEM. The dimensions of the features were measured using these micrographs by averaging three different measurements of the diameter of each feature.

### 3. Results and discussion

The first step in the ECMM with ultrashort voltage pulses of any material is the determination of a suitable electrolyte and potentials for machining. As previously discussed, pure Mo and Hastelloy B-2 and alloys are known to transpassively dissolve at easily accessible potentials in HCl electrolytes, [10–12,17]. Potentiodynamic scans were performed and the results of a scan for Hastelloy B-2 in deaerated 1 mol/L HCl are shown in Fig. 3.

Based on the potentiodynamic polarization curve, 1 mol/L HCl was chosen as an electrolyte because of the steep increase in anodic current as the potential was increased past the passive regime. This indicated transpassive dissolution of the Hastelloy B-2. Visual inspection of the sample following the scan indicated that the sample was indeed reacting under these conditions as the surface

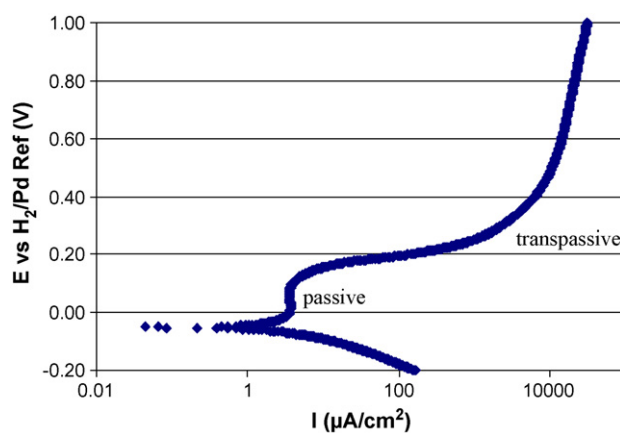


Fig. 3. Potentiodynamic scan of Hastelloy B-2 in 1 M HCl. The steep increase in anodic current density as the potential was increased indicated the transpassive dissolution of the Hastelloy B-2. This was desirable for use in ECMM as the workpiece can be held at potentials above open circuit, but below the transpassive regime unless pulsed by the tool.

appeared to be dissolved and was slightly roughened. The solution around the electrode had a yellow color attributed to dissolved Mo, likely as  $\text{HMoO}_4^-$  [17,19]. Aerated 1 mol/L and 2 mol/L HCl electrolyte were also examined and their potentiodynamic scans were found to have similar  $I$ - $V$  behavior, although the passive regime was obscured by the oxygen reduction reaction.

The DC potential of the substrate,  $U_{\text{Sub}}$ , was chosen slightly anodic of open circuit, as this was found to work well when used previously with Ni substrates [3], but suitably low to stay below the steep increase of anodic current density. The DC “off” potential of the tool,  $U_{\text{Tool}}$ , was then chosen to be slightly positive of the substrate potential. Care must be taken not to bias the tool negative of the substrate, as this can cause redeposition of the machined material.

Following the determination of suitable machining conditions, a study was conducted on the effect of the pulse duration on the ECMM of Hastelloy B-2 workpieces. In this study microfeatures were machined into Hastelloy B-2 workpieces to a depth of approximately 3  $\mu\text{m}$  using both 1 mol/L and 2 mol/L HCl. The diameter of the tool used in this study was 5  $\mu\text{m}$ . The average feed speed or machining rate of the tool was 1.8  $\mu\text{m}/\text{min}$  and four sets of four features with pulse durations of 200 ns, 100 ns, 50 ns, and 25 ns were machined with the same tool. The average diameter, average gap width, and standard deviation of the gap width for this study are shown in Table 1. The gap width is defined here as in previous ECMM work [3] as half the difference of the feature diameter and the tool diameter. Thus, the gap width is a measure of the resolution of the machining. As shown in Table 1, the gap width decreased with shorter pulse durations for both electrolyte concentrations. Representative examples of these results machined with 1 mol/L HCl at the four pulse durations studied are shown in Fig. 4.

An analogous study was performed machining microfeatures into Hastelloy B-2 workpieces to a depth of 10  $\mu\text{m}$  with 1 mol/L and 2 mol/L HCl. The diameter of the tool used in this study was 15  $\mu\text{m}$  and the average machining rate was 1.8  $\mu\text{m}/\text{min}$ . Once again the gap width decreased with shorter pulse duration as shown in Table 2. These results are confirmed visually by the data shown in Fig. 5.

In Fig. 6 the gap width of the holes machined to 3  $\mu\text{m}$  and 10  $\mu\text{m}$  is plotted vs. pulse duration, further illustrating the effects of pulse duration, total machining time, and solution concentration. As expected from Tables 1 and 2, Fig. 6 shows that shorter pulse duration leads to smaller gap widths and higher machining resolution. It also demonstrates the effect of the total machining time on

**Table 1**

The average diameter, gap width, and standard deviation of the gap width for the microstructures machined to a depth of 3  $\mu\text{m}$  into a Hastelloy B-2 workpiece with a 5  $\mu\text{m}$  tool using 1 mol/L and 2 mol/L HCl. The gap width is a measure of the resolution of the ECM. The gap width = (average diameter – tool width)/2, and the standard deviation of the gap was calculated from three gap width determinations made using different hole cross-sections.

Electrolyte	Pulse duration (ns)	Average diameter ( $\mu\text{m}$ )	Gap width ( $\mu\text{m}$ )	Standard deviation of gap ( $\mu\text{m}$ )
1 mol/L HCl	200	48.7	21.9	1.00
	100	28.6	11.8	2.96
	50	17.7	6.3	0.32
	25	9.4	2.2	0.60
2 mol/L HCl	200	39.0	17.0	2.05
	100	29.6	12.3	1.68
	50	18.0	6.5	1.36
	25	12.1	3.6	0.75

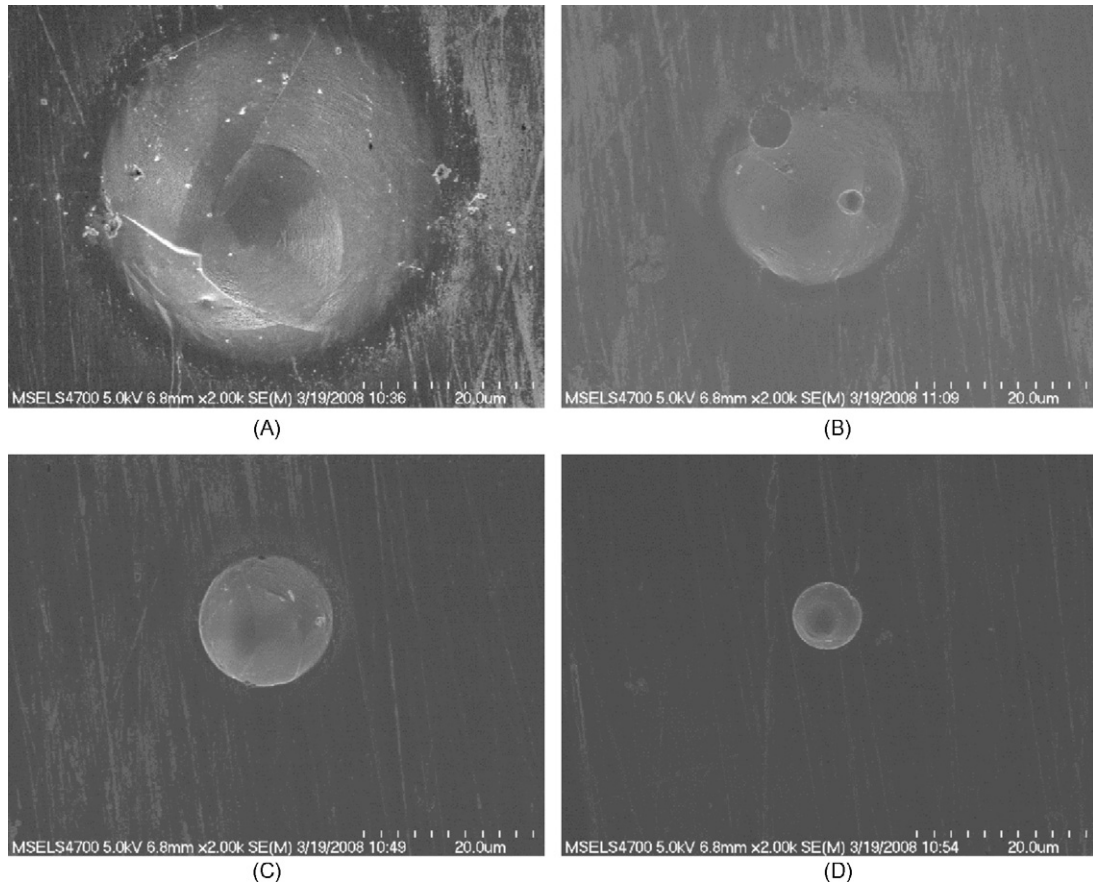


**Fig. 4.** Scanning electron micrographs of features machined 3  $\mu\text{m}$  into Hastelloy B-2 using a 5  $\mu\text{m}$  tool. Experimental conditions—electrolyte: 1 mol/L HCl, pulse amplitude: 1.3 V,  $U_{\text{Sub}}$ : +0.1 V,  $U_{\text{Tool}}$ : +0.2 V, and pulse duration: (A) 200 ns, (B) 100 ns, (C) 50 ns, (D) 25 ns.

the resolution as the reaction spreads over larger lateral distances of the substrate as machining time is increased to go from 3  $\mu\text{m}$  deep holes to 10  $\mu\text{m}$  deep holes. The rate at which this occurs is primarily dependent on the pulse duration. This effect is evident

in the increasingly larger difference between the 3  $\mu\text{m}$  deep holes and 10  $\mu\text{m}$  deep holes at longer pulse durations in Fig. 6. In terms of solution concentration Fig. 6 does not show a significant difference between the gap widths of the features machined at 1 mol/L

**Table 2**

The average diameter, average gap width, and standard deviation of the gap width for the microstructures machined to a depth of 10  $\mu\text{m}$  into a Hastelloy B-2 workpiece with a 15  $\mu\text{m}$  tool in 1 mol/L and 2 mol/L HCl.

Electrolyte	Pulse duration (ns)	Average diameter ( $\mu\text{m}$ )	Gap width ( $\mu\text{m}$ )	Standard deviation of gap ( $\mu\text{m}$ )
1 mol/L HCl	200	100.3	42.6	7.60
	100	62.2	23.6	7.80
	50	32.2	8.6	1.94
	25	18.1	1.5	1.23
2 mol/L HCl	200	96.0	40.5	1.52
	100	55.4	20.2	3.25
	50	30.7	7.8	1.23
	25	18.4	1.7	0.42

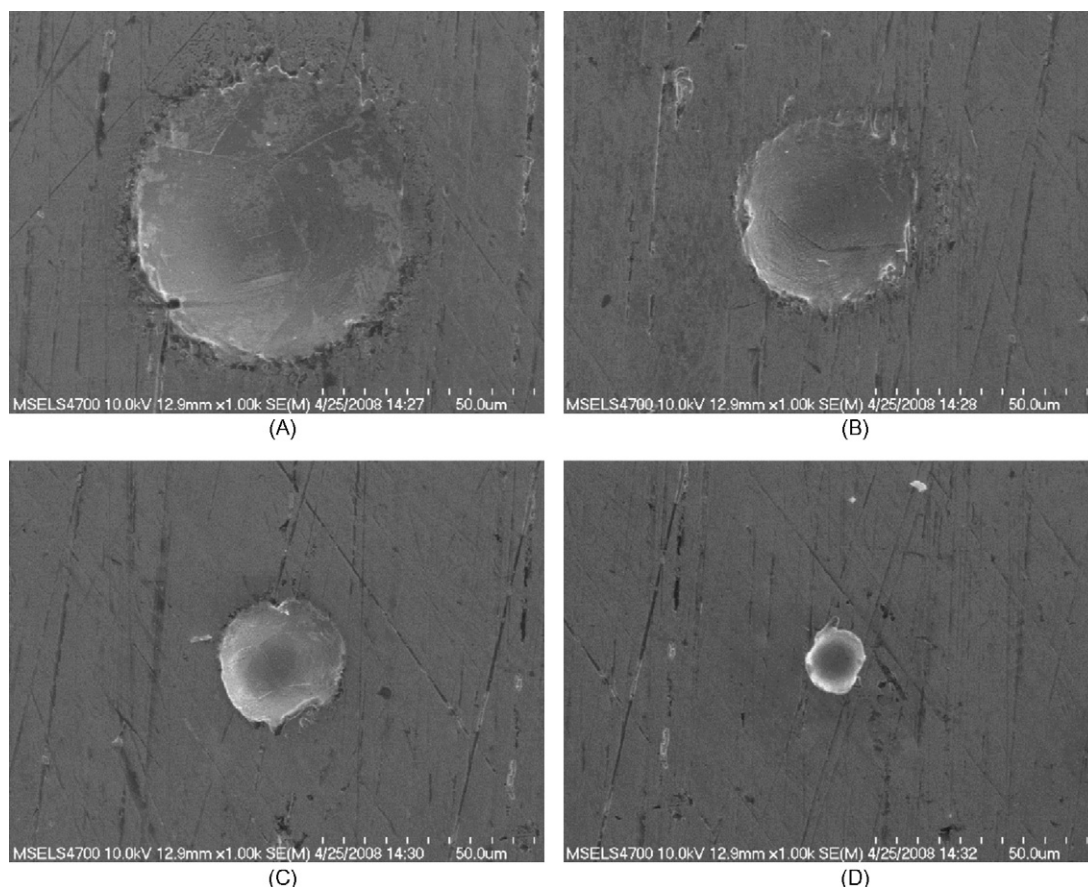


**Fig. 5.** Scanning electron micrographs of features machined 10  $\mu\text{m}$  into Hastelloy<sup>®</sup> B-2<sup>®</sup> using a 15  $\mu\text{m}$  tool. Experimental conditions—electrolyte: 1 mol/L HCl, pulse amplitude: 1.3 V,  $U_{\text{Sub}}$ : +0.1 V,  $U_{\text{Tool}}$ : +0.2 V, and pulse duration: (A) 200 ns, (B) 100 ns, (C) 50 ns, (D) 25 ns.

and 2 mol/L HCl, which is due to the relatively high conductivity of the HCl solutions used to machine these features. If more dilute solutions were used the gap width would likely decrease with decreasing solution concentration as demonstrated in previous ECMM work [3].

A study investigating the use of ECMM with ultrashort pulses for the fabrication of higher aspect ratio features on Hastelloy B-2 workpieces was also undertaken. In this study the workpieces were ground to a thickness of approximately 100  $\mu\text{m}$ . This was

done to allow the machined feature to penetrate the surface of the workpiece, so that the depth of the machining could be visually confirmed. The tool electrode employed in the machining of the deep features had uniform diameter of 40  $\mu\text{m}$  down its shaft, after the initial “tip” that extended out for the first 20  $\mu\text{m}$ , and is shown in Fig. 7. An example of a feature machined with 100 ns pulses through the 100  $\mu\text{m}$  workpiece is shown in Fig. 7. This feature had a diameter of slightly larger than 50  $\mu\text{m}$ , thus the aspect ratio of this feature was nearly 2:1. The hole diameter was found

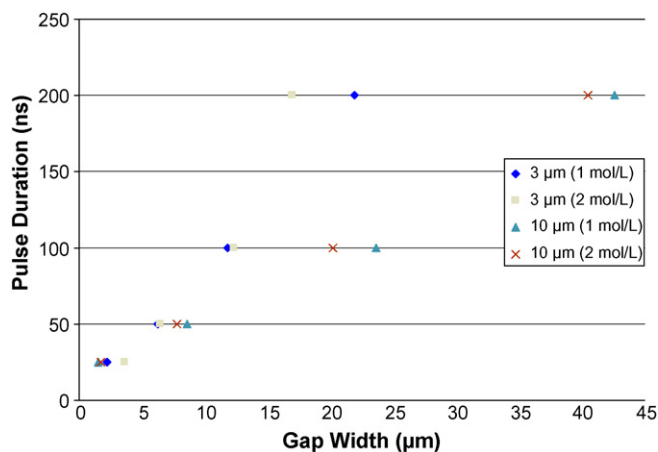


**Fig. 6.** Gap width vs. pulse duration for the results displayed in Tables 1 and 2. The effect of the pulse duration on the machining resolution at longer machining times is demonstrated by the increasing difference in gap width between the 3  $\mu\text{m}$  deep holes and the 10  $\mu\text{m}$  deep holes at the longer pulse durations.

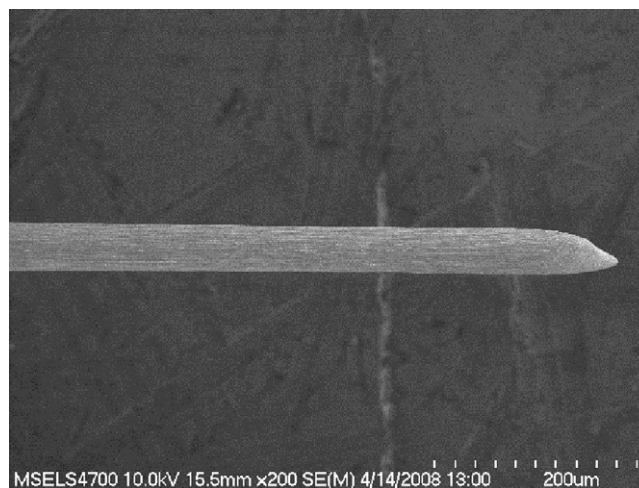


**Fig. 7.** Scanning electron micrograph of the W tool electrode used to machine the feature shown in Fig. 8.

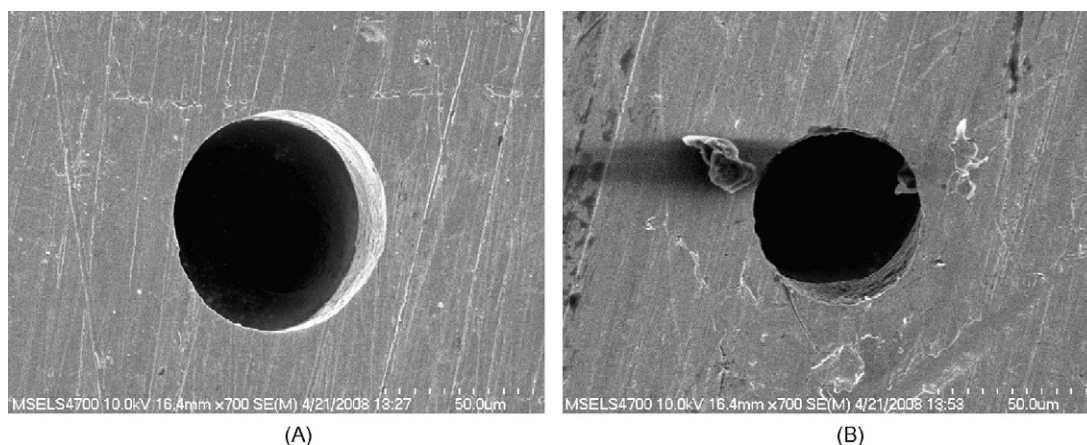


**Fig. 8.** Scanning electron micrograph of the second of the features machined 100  $\mu\text{m}$  into Hastelloy<sup>®</sup> B-2<sup>®</sup> using the W tool shown in Fig. 6. Experimental conditions—pulse duration: 100 ns, electrolyte: 1 mol/L HCl, pulse amplitude: 1.5 V,  $U_{\text{Sub}}$ : +0.1 V,  $U_{\text{Tool}}$ : +0.2 V. (A) The side of the Hastelloy sample on which the tool entered. (B) The opposite side of the Hastelloy where the tool emerged after machining through the sample.

to be slightly larger at the top of the hole, on the side where the machining was started. Since the tool diameter was approximately constant across the length used for this machining operation, this is evidence that the Hastelloy continued to etch at the top of the hole at a reduced rate during machining. Although the interior of the hole could not be examined changes to the hole was not examined.

In order to machine the feature shown in Fig. 8, progressively slower feed speeds were used as the tool was fed deeper into the Hastelloy B-2 because of a decrease in the rate of the anodic dissolution reaction. This decrease in reaction rate as the tool entered the surface was even more pronounced in attempts to machine a feature through the workpiece with 50 ns pulses. In this case, the 30 nm increments that represented the lowest resolution of the positioning system would cause the tip to crash, since the reaction was proceeding too slowly to keep up with the advancement of the tool position.

The decrease in the reaction rate is due to a decrease in flux of the reaction products out of the gap between the tool and the machined feature. As an example of how this happens, consider the feature shown in Fig. 8 machined with 100 ns pulses, 1 mol/L HCl, and using the tool shown in Fig. 7. The diameter of this feature is slightly larger than 50  $\mu\text{m}$ , thus the gap width between the tool and the walls of the feature is approximately 5  $\mu\text{m}$ . As the feature is machined to greater depths, the reaction products,  $\text{Ni}^{2+}$  and likely  $\text{HMoO}_4^-$  [17], will begin to build up in this gap as it will take them longer to diffuse out of the gap. This will slow down the anodic reaction, as a progressively larger boundary layer will be formed around the machined feature, resulting in a decrease in the current density, thus slowing the anodic dissolution. The same phenomenon is seen in standard electrochemical machining (ECM) techniques [20,21], where jets are used to increase the flow rate of the electrolyte inside the electrode–workpiece gap.

If the rate of the anodic dissolution could be maintained at larger depths, the fabrication of higher aspect ratio microstructures on Hastelloy B-2 workpieces would be readily achievable through the use of pulse durations shorter than 50 ns. The evolution of the feature profile as a function of pulse duration has been modeled by Kenney et al. [22–24]. These shorter pulse durations are currently inaccessible for deep features as the tool–workpiece gap is too small to allow for adequate flux of the reaction products out of the gap. It is proposed that if the tool could be withdrawn from the feature at regular intervals, it would allow for fresh electrolyte to flush the gap as it undergoes ECMM, and the anodic dissolution would be suitably fast at large feature depths. Flushing this gap has been

used previously in ECMM, and the influence of the flushing on the anodic dissolution was also discussed [6].

#### 4. Conclusions

The maskless process, ECMM with ultrashort voltage pulses, was used to create microstructures on the corrosion resistant material Hastelloy B-2 using a new experimental apparatus consisting of standard electrochemical equipment combined with a custom electrical circuit that was constructed easily and at low cost. Microstructures were machined while controlling the size of the structures through the combination of the size of the microscale tool electrode, the duration of the ultrashort pulses, and the depth to which the features were machined. The results clearly demonstrated that the size resolution of the ECMM process on Hastelloy B-2 workpieces is largely dependent on the pulse duration. The ECMM through 100  $\mu\text{m}$  thick Hastelloy B-2 workpieces resulted in a microstructure with an aspect ratio approaching 2:1, and indicates the potential for the fabrication of higher aspect ratio structures than have been achieved previously with this technique. The use of this method to create microstructures on Hastelloy B-2 has demonstrated that ECMM with ultrashort voltage pulses is a viable strain-free process for microfabrication on industrially relevant materials.

#### Acknowledgments

The authors would like to acknowledge David Kelley of NIST for help in preparing the Hastelloy B-2 workpieces, Dr. Liang Yueh Ou Yang of NIST for his help preparing the tool electrodes, and Dr. John Bonevich and Dr. Chang Hwa Lee of NIST for their assistance with the SEM. J.J. Maurer and J.L. Hudson would also like to acknowledge the National Institute of Standards and Technology Research Grant # SB1341-07-CN-0047 for support for this research.

#### References

- [1] R. Schuster, V. Kirchner, X.H. Xia, A.M. Bittner, G. Ertl, *Physical Review Letters* 80 (1998) 5599.
- [2] R. Schuster, V. Kirchner, P. Allongue, G. Ertl, *Science* 289 (2000) 98.
- [3] A.L. Trimmer, M. Kock, R. Schuster, J.L. Hudson, *Applied Physics Letters* 82 (2003) 3327.
- [4] V. Kirchner, X.H. Xia, R. Schuster, *Accounts of Chemical Research* 34 (2001) 371.
- [5] V. Kirchner, L. Cagnon, R. Schuster, G. Ertl, *Applied Physics Letters* 79 (2001) 1721.
- [6] M. Kock, V. Kirchner, R. Schuster, *Electrochimica Acta* 48 (2003) 3213.
- [7] M.T. Giacomini, R. Schuster, *Physical Chemistry Chemical Physics* 7 (2005) 518.

- [8] P. Allongue, P. Jiang, V. Kirchner, A.L. Trimmer, R. Schuster, *Journal of Physical Chemistry B* 108 (2004) 14434.
- [9] A.L. Trimmer, J.J. Maurer, R. Schuster, G. Zangari, J.L. Hudson, *Chemistry of Materials* 17 (2005) 6755.
- [10] W.Z. Friend, *Corrosion of Nickel and Nickel-Base Alloys*, Wiley-Interscience, New York, 1980.
- [11] T.P. Moffat, R.M. Latanision, R.R. Ruf, *Journal of the Electrochemical Society* 138 (1991) 3280.
- [12] D.A. Jones, *Principles and Prevention of Corrosion*, Macmillan Publishing Company, New York, 1992.
- [13] A.M. Rouhi, *Chemical and Engineering News* (2004) 82.
- [14] H.H. Uhlig, P. Bond, H. Feller, *Journal of the Electrochemical Society* 110 (1963) 650.
- [15] J. Horvath, H.H. Uhlig, *Journal of the Electrochemical Society* 115 (1968) 791.
- [16] J.L. Luo, M.B. Ives, *Journal of the Electrochemical Society* 144 (1997) 3907.
- [17] Y.C. Lu, C.R. Clayton, *Corrosion Science* 29 (1989) 927.
- [18] J.P. Hoare, S. Schuldiner, *Journal of Physical Chemistry* 61 (1957) 399.
- [19] M. Pourbaix, *Atlas of Electrochemical Equilibria in Aqueous Solutions*, National Association of Corrosion Engineers, Houston, 1966.
- [20] M. Datta, *IBM Journal of Research and Development* 42 (1998) 655.
- [21] D. Landolt, P.-F. Chauvy, O. Zinger, *Electrochimica Acta* 48 (2003) 3185.
- [22] J.A. Kenney, G.S. Hwang, W. Shin, *Applied Physics Letters* 84 (2004) 3774.
- [23] J.A. Kenney, G.S. Hwang, *Nanotechnology* 16 (2005) S309.
- [24] J.A. Kenney, G.S. Hwang, *Electrochemical and Solid-State Letters* 9 (2006) D1.